Inelastic neutron scattering study of spin waves in the garnet $Mn_3Al_2Ge_3O_{12}$ with a triangular magnetic structure

1999 J. Phys.: Condens. Matter 11 2869

(http://iopscience.iop.org/0953-8984/11/14/003)

J. Phys.: Condens. Matter **11** (1999) 2869–2878. Printed in the UK PII: S0953-8984(99)99819-3

Inelastic neutron scattering study of spin waves in the garnet $Mn_3Al_2Ge_3O_{12}$ with a triangular magnetic structure

A Gukasov†¶, V P Plakhty‡, B Dorner§, S Yu Kokovin‡,
V N Syromyatnikov‖, O P Smirnov‡ and Yu P Chernenkov‡

† Laboratoire Léon Brillouin, CE Saclay, 91191 Gif sur Yvette, France
‡ Petersburg Nuclear Physics Institute, Gatchina, St Petersburg 188350, Russia
§ Institut Laue–Langevin, 156X, F-38042 Grenoble Cédex 9, France
‖ Institute for Metal Physics of the Ural Scientific Centre, Ekaterinburg 620219, Russia

Received 1 December 1998

Abstract. The spin-wave spectrum of the antiferromagnet $Mn_3Al_2Ge_3O_{12}$ with the garnet structure has been studied by inelastic neutron scattering on the triple-axis spectrometers IN12 and IN14 at ILL. Magnon dispersion curves were measured along [ξ ξ 0] and [ξ ξ ξ] directions up to energies of 0.3 THz. The spin-wave symmetry analysis, which reduced the number of independent exchange parameters to six, was performed to ensure correct description of the spin-wave branches. As determined by the fitting, five of the parameters are statistically significant and have been found to be $J_1 = -0.70(2)$ K, $J_2 = -0.08(2)$ K, $J_3 = -0.25(2)$ K, $J_4 = -0.20(2)$ K and $J_5 = -0.07(2)$ K. This quite unusual sequence of exchange parameters clearly demonstrates the importance of the superexchange chain geometry.

1. Introduction

Spin dynamics of antiferromagnetic garnets attracts considerable interest, due to the possibility of synthesizing a large family of compounds having different 3d ions (Fe, Cr, Mn) at octahedral (a), dodecahedral (c) and tetrahedral (d) sites of the garnet unit cell. An interesting feature of these garnets is an interaction of the 3d ions via superexchange paths that involve at least two successively arranged oxygen ions. Depending on the type of magnetic 3d ion and the site which it occupies in the garnet unit cell, a large variety of antiferromagnetic structures were observed at low temperatures. (For a review, see reference [1].) Systematic investigations of these garnets are therefore very helpful for the understanding of the superexchange mechanism when more than one non-magnetic ion is involved.

In our previous work, the spin dynamics of the collinear antiferromagnets $Ca_3Fe_2Ge_3O_{12}$, $Ca_3Cr_2Ge_3O_{12}$ and $Ca_3Fe_2Si_3O_{12}$ with the magnetic ions at the a sites were investigated [2–5]. Since the number of magnetic ions in these garnets is large (eight in the primitive unit cell) the observed magnon spectra for these compounds were rather complicated (eight magnon branches were found for $Ca_3Fe_2Ge_3O_{12}$ and $Ca_3Fe_2Si_3O_{12}$ and four branches for $Ca_3Cr_2Ge_3O_{12}$). It has been shown, however, that due to the high symmetry of the garnet structure these magnon spectra can be perfectly described by a model based on linear spin-wave theory [6] containing only three exchange parameters. Further analysis of the exchange parameters for the two isomorphous compounds $Ca_3Fe_2Ge_3O_{12}$ and $Ca_3Fe_2Si_3O_{12}$ obtained

¶ Fax: +33-169-08-82-61; e-mail address: gukasov@bali.saclay.cea.fr.

0953-8984/99/142869+10$19.50

by refinement of the model allowed us to identify the main superexchange paths via p_σ orbitals of the intermediate oxygen atoms and to obtain information about the evolution of exchange parameters with the distance between maxima of the p_σ lobes.

As a continuation of these studies, the spin-wave spectrum of the c-sublattice garnet $Mn_3Al_2Ge_3O_{12}$ has been investigated, and the results are presented in this paper. The difference from the case of the garnets containing the 3d ions at a sites is that the superexchange path between the nearest neighbours includes only one oxygen ion. Nevertheless the Néel temperature (6.8 K) of this compound is about half of that the a-sublattice garnets. Therefore its typical spin-wave (SW) energies should be on average smaller as well. Taking into account the large number (twelve) of magnetic atoms in the c sublattice and the non-collinear magnetic structure, a considerably more complicated magnon spectrum was expected as compared to those of the a-sublattice garnets. This should lead to a strong overlapping of different spin-wave branches, which in turn sometimes prevents one from attributing the measured SW frequency to a definite branch. To overcome all of these difficulties a new approach was needed allowing one, first, to choose the special points and the symmetry directions of the Brillouin zone (BZ) with the highest degeneracy, where the analytical solutions for the SW frequencies could be obtained, and second, to determine the number of independent exchange parameters and to refine their values by comparison with the experimental spectra. Below we shall describe the procedures of SW symmetry analysis and numerical calculations which allow us to accomplish this task.

2. Magnetic structure and spin-wave symmetry analysis

In the body-centred cubic unit cell described by the space group $Ia3d$, the Mn^{2+} ions occupy the symmetry position 24c. Half of the atoms are contained in the primitive unit cell of the garnet and their coordinates can be written as follows:

1: (1/8 0 1/4)	**2**: (1/4 1/8 0)	**3**: (0 1/4 1/8)
4: (3/8 0 3/4)	**5**: (3/4 3/8 0)	**6**: (0 3/4 3/8)
7: (5/8 0 1/4)	**8**: (1/4 5/8 0)	**9**: (0 1/4 5/8)
10: (7/8 0 3/4)	**11**: (3/4 7/8 0)	**12**: (0 3/4 7/8).

Each group of three atoms with the coordinates written down in the same line are transformed into each other by rotation about a threefold axis.

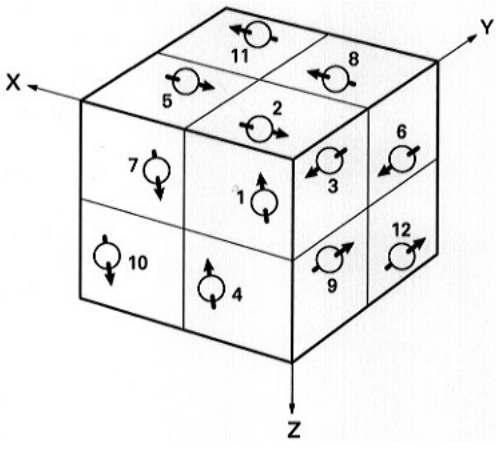

Figure 1. The magnetic structure of $Mn_3Al_2Ge_3O_{12}$. The spins are along directions of the type $[-2\ 1\ 1]$. The spins of atoms inside the unit cell are connected with the ones shown by the translation $t = [1/2\ 1/2\ 1/2]$.

The $Mn_3Al_2Ge_3O_{12}$ garnet orders antiferromagnetically at $T_N = 6.8$ K, with the magnetic moment of 3.98(12) μ_B per Mn atom. According to [7, 8] its magnetic unit cell coincides with the chemical one (the propagation vector $\boldsymbol{k} = 0$) and consists of six triangularly arranged antiferromagnetic sublattices with magnetic moments along one of the directions of the [−2 1 1] type:

$$\boldsymbol{S}_1 = \boldsymbol{S}_4 = -\boldsymbol{S}_7 = -\boldsymbol{S}_{10} = S(1\ 1\ -2) \tag{1}$$

$$\boldsymbol{S}_2 = \boldsymbol{S}_5 = -\boldsymbol{S}_8 = -\boldsymbol{S}_{11} = S(-2\ 1\ 1) \tag{2}$$

$$\boldsymbol{S}_3 = \boldsymbol{S}_6 = -\boldsymbol{S}_9 = -\boldsymbol{S}_{12} = S(1\ -2\ 1). \tag{3}$$

The magnetic structure is shown in figure 1. The spin directions of the rest of the twelve atoms inside the body-centred cubic unit cell are obtained from $\boldsymbol{S}_1, \ldots, \boldsymbol{S}_{12}$ by a translation $t = [1/2\ 1/2\ 1/2]$. A weak spin component arranged antiferromagnetically has been found in reference [8], but its value is within the limits of three standard deviations, and we neglect it as in reference [7].

In the present work numerical and analytical methods of SW analysis were used. The numerical calculations, valid for non-collinear magnetic structures, were developed on the basis of a general SW symmetry analysis method described in references [9, 10]. A Fortran program had been written, which determines for given moment directions the magnetic space group, finds the SW representation and performs the symmetrization of the SW Hamiltonian (H^{SW}). At this stage either the numerical calculations of the SW frequencies and eigenfunctions were performed, or the analytical method was applied for special symmetry points, which consisted in the diagonalization of H^{SW} using SW irreducible representations.

The SW irreducible representations are usually constructed using the magnetic space group (MSG) [9, 10]. It is known however that for crystals containing many magnetic atoms in the primitive unit cell the symmetrization of H^{SW} based on the MSG is not very efficient since many elements of H^{SW} remain independent. It is more useful to neglect weak interactions resulting in small splittings of the SW branches and to find the approximate spectra. This can be done within the exchange approximation for the spin-wave Hamiltonian [11]. The symmetry analysis was performed using the stabilizer concept proposed in references [10, 11].

We shall summarize below the main features of the predicted SW spectrum. The exchange P-type colour group [11] of the structure shown in figure 1 can be written as

$$\mathrm{P} = \mathrm{T}_d^6 + h'_{25}\mathrm{T}_d^6. \tag{4}$$

Following the procedure described in detail in references [10, 11] the SW representation (d_{SW}) for the centre of the Brillouin zone in $Mn_3Al_2Ge_3O_{12}$ can be reduced to the following representations:

(i) Γ point; $\boldsymbol{k}_{11} = 0$; T192:

$$d_{SW}^{\Gamma} = 2\{\tau_1(1) \oplus \tau_2(1) \oplus 2\tau_3(2) \oplus \tau_4(3) \oplus \tau_5(3)\} \tag{5}$$

where the $\tau_i(n)$ are irreducible representations in Kovalev's notation [12] (i and n are the number and the dimension of the representation, respectively). These representations are given in the table T192 of reference [12]. Similar reductions for the other symmetry points and lines in the Brillouin zone are given below together with the numbers of the corresponding tables in reference [12].

(ii) H point; $\boldsymbol{k}_{12} = (0\ 0\ 1)2\pi/a$; T232:

$$d_{SW}^{H} = 2\{\tau_1(1) \oplus \tau_2(1) \oplus 2\tau_3(2) \oplus \tau_4(3) \oplus \tau_5(3)\}. \tag{6}$$

(iii) P point; $\boldsymbol{k}_{10} = (1/2\ 1/2\ 1/2)2\pi/a$; T231:

$$d_{SW}^{P} = 2\{\tau_1(2) \oplus \tau_2(2) \oplus 2\tau_3(4)\}. \tag{7}$$

(iv) N point; $\boldsymbol{k}_9 = (0\ 1/2\ 1/2)2\pi/a$; T230:

$$d_{\mathrm{SW}}^{\mathrm{N}} = 2\{6\tau_1(2)\}. \tag{8}$$

(v) Δ line; $\boldsymbol{k}_8 = (0\ 0\ \mu)2\pi/a$; T126:

$$d_{\mathrm{SW}}^{\Delta} = 2\{3\tau_1(1) \oplus 3\tau_2(1) \oplus 3\tau_3(1) \oplus 3\tau_4(1)\}. \tag{9}$$

(vi) Σ line; $\boldsymbol{k}_4 = (0\ \mu\ \mu)2\pi/a$; T118:

$$d_{\mathrm{SW}}^{\Sigma} = 2\{6\tau_1(1) \oplus 6\tau_2(1)\}. \tag{10}$$

(vii) Δ line; $\boldsymbol{k}_7 = (\mu\ \mu\ \mu)2\pi/a$; T191:

$$d_{\mathrm{SW}}^{\Lambda} = 2\{2\tau_1(1) \oplus 2\tau_2(1) \oplus 4\tau_3(2)\}. \tag{11}$$

As follows from these equations, the highest degeneracy of SW spectra occurs at the symmetry points Γ, H (six branches) and P (four branches), where the analytical expressions for SW frequencies can be obtained, and along the Δ line (eight branches) where the solutions can be obtained only for representations $\tau_1(1)$ and $\tau_2(1)$, while the $\tau_3(2)$ representation will be characterized by a secular equation of the eighth power. In contrast, the SW spectra along the Δ and Σ lines each consist of twelve branches and can hardly be suitable for any interpretation, taking into account the complexity of the magnetic structure and the unpredictable character of the superexchange interaction via double oxygen bonds. Therefore in our experiment special attention was paid to the measurements along the Δ line and at the three high-symmetry points (Γ, P and H).

We note also that a similar analysis based directly on the MSG gives eight branches at the Γ, P, H points and along the Δ line and twelve branches in all other symmetry directions. No analytical solution for SW frequencies can be obtained in these cases, confirming that using the MSG is not very efficient in interpretations of the spin waves in the complex magnetic structures, since the number of predicted SW branches is simply equal to the number of magnetic atoms in the primitive unit cell.

Table 1. The SW modes of $Mn_3Al_2Ge_3O_{12}$ at the Γ point. $\varepsilon = \exp(\mathrm{i}\,2\pi/3)$, $\varepsilon^* = \exp(-\mathrm{i}\,2\pi/3)$.

	Atom number in the primitive unit cell											
	1	2	3	4	5	6	7	8	9	10	11	12
τ_1	1	1	1	1	1	1	1	1	1	1	1	1
τ_2	1	1	1	1	1	1	−1	−1	−1	−1	−1	−1
τ_3	1	ε	ε^*	1	ε	ε^*	0	0	0	0	0	0
	0	0	0	0	0	0	ε	1	ε^*	ε	1	ε^*
τ_3'	0	0	0	0	0	0	1	ε	ε^*	1	ε	ε^*
	1	ε^*	ε	1	ε^*	ε	0	0	0	0	0	0
τ_4	1	0	0	−1	0	0	−1	0	0	1	0	0
	0	1	0	0	−1	0	0	−1	0	0	1	0
	0	0	1	0	0	−1	0	0	−1	0	0	1
τ_5	1	0	0	−1	0	0	1	0	0	−1	0	0
	0	1	0	0	−1	0	0	1	0	0	−1	0
	0	0	1	0	0	−1	0	0	1	0	0	−1

To illustrate the possibilities of symmetry analysis we shall present the results of the analytical calculation of the SW spectra at the Γ point. The spin-wave modes (SWM) at the Γ point of $Mn_3Al_2Ge_3O_{12}$, which are shown in table 1, have been obtained using the stabilizer method [9]. We should draw attention to the remarkable efficiency of the method in our case. This is due to the simple fact that instead of using all 24 symmetry elements of the magnetic group, namely g_1–g_{12} and g_{37}–g_{48}, in the SWM calculations, only the first-atom stabilizer elements (g_1, g_2) were used. The SWM for the other atoms have been obtained by the action of the representative symmetry elements on the first atom.

As a next step, the symmetrization of the Hamiltonian $H^{SW} = -\Sigma_{ij} J_{ij} S_i S_j$ was performed using H^{SW} in a block-matrix form, where the block elements were denoted in a standard form [11] as

$$H_{ij} = \begin{pmatrix} B_{ij}(q) & A_{ij}(q) \\ A^*_{ij}(-q) & B^*_{ij}(-q) \end{pmatrix} \qquad i, j = 1, \ldots, 12 \tag{12}$$

and i, j are magnetic atom numbers in the primitive unit cell of garnet. It follows from the symmetrization that H^{SW} contains only six independent elements and can be written as

$$H^{SW}_{ij} = \begin{pmatrix} a & b & b^* & c & b & b^* & d & e & e^* & f & e & e^* \\ b^* & a & b & b^* & c & b & e^* & d & e & e^* & f & e \\ b & b^* & a & b & b^* & c & e & e^* & d & e & e^* & f \\ c & b & b^* & a & b & b^* & f & e & e^* & d & e & e^* \\ b^* & c & b & b^* & a & b & e^* & f & e & e^* & d & e \\ b & b^* & c & b & b^* & a & e & e^* & f & e & e^* & d \\ d & e^* & e & f & e^* & e & a & b^* & b & c & b^* & b \\ e & d & e^* & e & f & e^* & b & a & b^* & b & c & b^* \\ e^* & e & d & e^* & e & f & b^* & b & a & b^* & b & c \\ f & e^* & e & d & e^* & e & c & b^* & b & a & b^* & b \\ e & f & e^* & e & d & e^* & b & c & b^* & b & a & b^* \\ e^* & e & f & e^* & e & d & b^* & b & c & b^* & b & a \end{pmatrix} \tag{13}$$

where the block matrices

$$a = H_{1,1}(q) \qquad b = H_{1,2}(q) \qquad c = H_{1,4}(q)$$
$$d = H_{1,7}(q) \qquad e = H_{1,8}(q) \qquad f = H_{1,10}(q)$$

are constructed from the functions of the exchange integrals A_{ij}, B_{ij}, which can be found by performing a Hamiltonian transformation to the local coordinate systems. Such transformation gives

$$\begin{aligned} B_{11}(q) &= S(J_{11}(q) - J_{11}(0) + 2J_{12}(0) - J_{14}(0) + J_{17}(0) - 2J_{18}(0) + J_{1,10}(0)) \\ A_{11}(q) &= 0 \end{aligned} \tag{14}$$

$$B_{12}(q) = -\tfrac{1}{4} S J_{12}(q) \qquad A_{12}(q) = -\tfrac{3}{4} S J_{12}(q) \tag{15}$$

$$B_{14}(q) = S J_{14}(q) \qquad A_{14}(q) = 0 \tag{16}$$

$$B_{18}(q) = -\tfrac{3}{4} S J_{18}(q) \qquad A_{18}(q) = -\tfrac{1}{4} S J_{18}(q) \tag{17}$$

$$B_{1,10}(q) = 0 \qquad A_{1,10}(q) = -S J_{1,10}(q). \tag{18}$$

Next the diagonalization of H^{SW} was performed using the matrix constructed from the SWM given in table 1 and the SW frequencies ν have been found at the Γ point; these are given below:

$$\nu^2_{\tau_1} = \nu^2_{\tau'_3} = 0 \tag{19}$$

$$\nu^2_{\tau_2} = S^2(J_{12}(0) - J_{18}(0))(J_{17}(0) - 2J_{18}(0) + J_{1,10}(0)) \tag{20}$$

$$\nu^2_{\tau_3''} = \tfrac{1}{2}S^2(J_{12}(0) - J_{18}(0))(J_{17}(0) - 2J_{18}(0) + J_{1,10}(0)) \tag{21}$$

$$\nu^2_{\tau_4} = \nu^2_{\tau_5} = \tfrac{1}{3}S^2(J_{12}(0) - J_{14}(0) - J_{18}(0) + J_{1,10}(0))(J_{12}(0) - J_{14}(0) + J_{17}(0) - J_{18}(0)). \tag{22}$$

Here the $J_{ij}(\boldsymbol{q})$ are the Fourier components of the exchange parameters given in table 2 which is similar to a table in reference [13]. The values of the exchange parameters given in the table that correspond to the best fit will be discussed later on.

Table 2. The radii, R, of the coordination spheres and the corresponding independent exchange parameters, J_i, for the atoms 1 and j.

Number of sphere	R (Å)	j	J_i (K)
1	3.674	2, 3, 5, 6	$J_1 = -0.70(2)$
2	5.612	8, 9, 11, 12	$J_2 = -0.08(2)$
3	6.000	7	$J_3 = -0.25(2)$
4	6.708	10	$J_4 = -0.20(2)$
4	6.708	4	$J_5 = -0.07(2)$

Let us summarize the main features of the calculated SW spectrum. The one-dimensional representation τ_1 corresponds to the acoustic (Goldstone) SW mode and is degenerate with another acoustic mode described by the two-dimensional representation $\tau_{3'}$ (the degeneracy of these modes is lifted in the presence of an anisotropy). As follows from these equations, an additional degeneracy of the spin-wave branches occurs for the three-dimensional representations τ_4 and τ_5, decreasing the total number of SW branches from six to four. This degeneracy results from the colour exchange groups being based on the anisotropic exchange interaction symmetry, while in the equations above the isotropic exchange approximation was used, which brings an additional (higher) symmetry into the model. We note as well that the magnon frequencies of the τ_2- and τ_3'-representations are connected by the simple relation $\nu\tau_2 = \sqrt{2}\nu_{\tau_3''}$. Thus according to the above analysis the SW spectrum of $Mn_3Al_2Ge_3O_{12}$ at the Γ point consists of four branches (five branches in the presence of the staggered field anisotropy) and provides only two independent equations, which can be used to determine the exchange parameters.

A similar procedure applied to the P and H points has given three and two SW frequencies, respectively. As a result of such analysis six independent equations have been obtained, which could be used to determine starting values of the exchange parameters suitable for the further refinement of the model.

3. Experiment

The single crystal of $Mn_3Al_2Ge_3O_{12}$ had been grown from the melt by B V Mill' using the Czochralski method [14]. Its volume was about 1.5 cm^3. The Néel temperature (T_N) was determined by intensity measurements of the (1 1 0) antiferromagnetic reflection, and $T_N = 6.75$ K was obtained, in accordance with results known from the literature [7, 13]. The lattice constant was found to be 11.95 Å at 1.5 K. Inelastic neutron scattering experiments were performed on the IN3, IN12 and IN14 three-axis spectrometers at the ILL. The final wave vector k_f (incoming wave vector k_i, for IN12) was kept fixed at 1.3 Å^{-1}. The constant-$\boldsymbol{q}$ scans with k_i fixed were corrected for the varying analyser transmission by multiplying by $k_f^3 \cot\theta_A$. A cooled Be filter was used to reduce the higher-order contamination. The sample

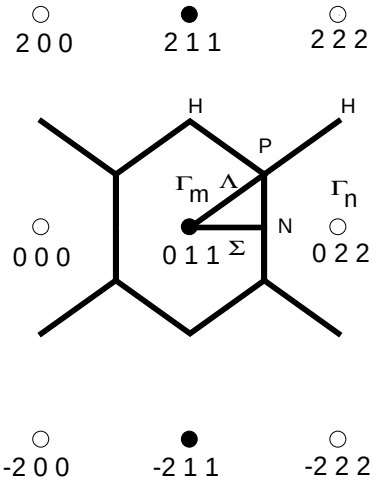

Figure 2. The plane of the reciprocal lattice investigated. Nuclear and magnetic reciprocal-lattice points are shown by open and closed circles, respectively.

was oriented with a [1 −1 0] axis vertical (see figure 2), and the measurements were carried out at 1.5 K in the [ξ ξ 0] and [ξ ξ ξ] directions.

A total of 133 magnon peaks were measured, including a large number of those at the different high-symmetry points (Γ, H, P) where the magnon peaks can be attributed unambiguously to a definite branch due to the high degeneracy of the spectra. To illustrate this, two magnon scans measured at the magnetic Γ_m point (0 1 1) and the nuclear, Γ_n point (0 2 2) are shown in figure 3. (We have introduced different Γ_m and Γ_n points for the sake of simplicity.) As seen from this figure, five SW branches are observed at the Γ_m, Γ_n points as compared to four branches predicted by the theory. As has been mentioned above, this disagreement is due to neglecting the magnetic anisotropy in the previous analysis, which is the cause of the splitting of two low-lying acoustic branches. (We note that the SW frequencies of the two lowest-lying modes, 0.04 and 0.071 THz, agree well with the AFMR results reported earlier [15].) We note as well that the acoustic branches of the spectrum have considerably higher

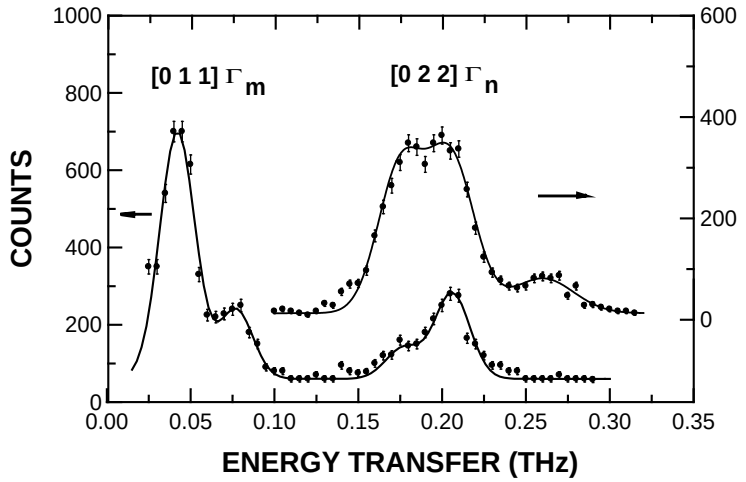

Figure 3. Some magnon groups measured at the points (0 1 1) and (0 2 2).

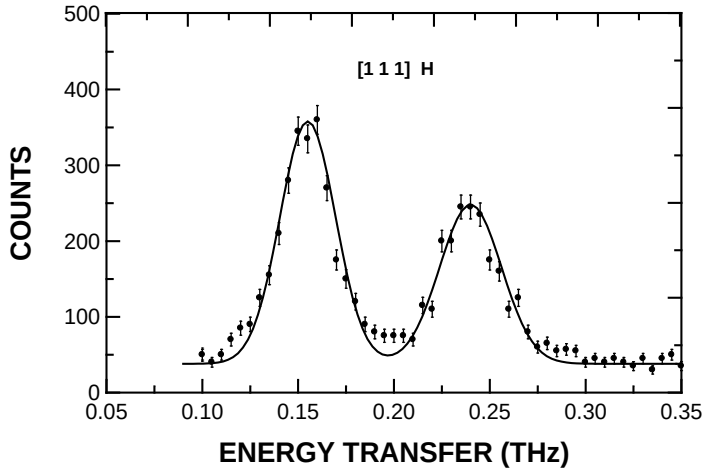

Figure 4. Magnon spectra measured at the H point (1 1 1).

intensities at the Γ_m point, while there are optic ones at the Γ_n point. Simple estimation shows that the ratio of the SW squared frequencies of the highest and the third mode is approximately equal to 2 in accordance with equations (20), (21). Thus the sequence of five SW frequencies at the Γ point can be presented as $\tau_3'(2)$, $\tau_1(1)$, $\tau_3''(2)$, $\tau_4(3) \oplus \tau_5(3)$, $\tau_2(1)$ with increasing energy, and the two highest frequencies can be used to calculate the exchange parameters using formulae (20), (22). Similar calculations have been performed for the H and P points. An example of SW spectra measured at the H point is shown in figure 4.

The results of the experiment are summarized in figure 5 where the measured SW dispersion is shown for two principal directions [ξ ξ ξ] and [ξ ξ 0]. Each experimental point in this figure represents in fact an average of several magnon peaks found at equivalent positions, and the error bars indicate the dispersion of magnon energy values around the average. The solid curves show the best least-squares fit to the data for the model taking into account the five exchange parameters $J_1, \ldots, J_5$ with the values indicated in table 2. These parameters have been refined using a least-squares routine that incorporated the program for numerical calculation of SW frequencies mentioned above. Since the magnon peaks can be attributed unambiguously to the high-symmetry points, only the data obtained at these points were used. The starting set of the exchange parameters was obtained from the analytical equations (20), (22) and similar equations for the symmetry points H and P.

4. Discussion

The spin-wave dispersion curves are determined for two directions, [ξ ξ ξ] and [ξ ξ 0], where the degeneracy allows their interpretation via a preliminary symmetry analysis including the stabilizer method [9] which happens to be very efficient in our case. Neglecting the area of low frequencies at small q-values where the crystalline anisotropy (which has not been considered) is of primary importance, the spin dynamics of $Mn_3Al_2Ge_3O_{12}$ is described rather well by the model that takes into account the superexchange interaction between the nearest neighbours (J_1) via one oxygen ion and all interactions via the chains with two successive oxygen ions. This means that four coordination spheres have been considered.

Altogether five exchange parameters have been obtained as explained above. Their values

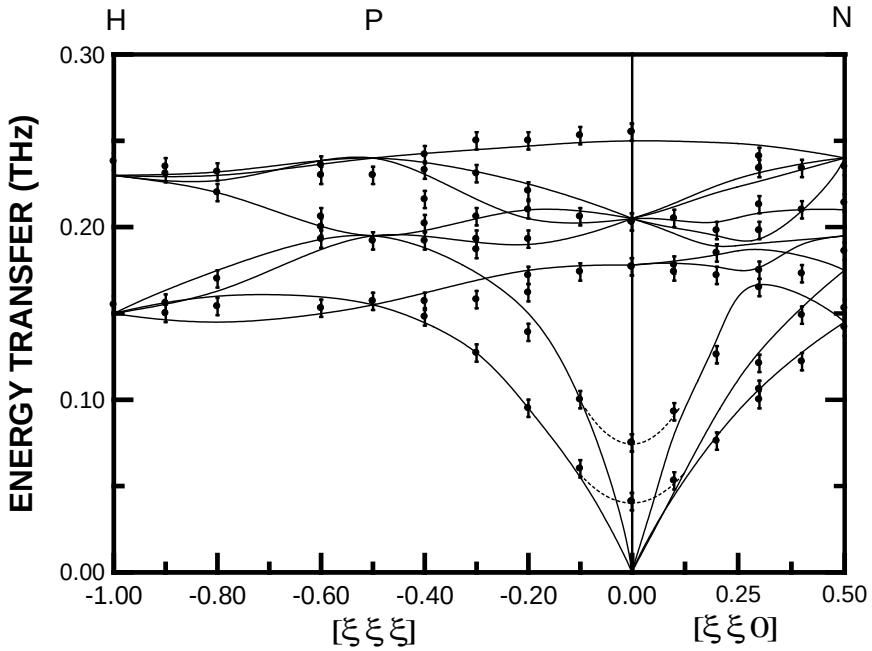

Figure 5. The dispersion curves in [ξ ξ ξ] and [ξ ξ 0] directions. Each point is an average for several magnon frequencies measured at equivalent positions. The solid curves represent the best fit over the experimental frequencies at the Γ, H, P points. The dotted curves around the Γ point show the gap in the SW spectrum due to anisotropy.

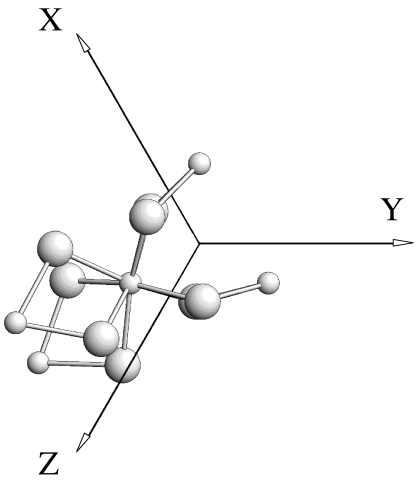

Figure 6. Superexchange paths (J_1) between Mn1 (crystallographic position (1/8 0 1/4)) and its four nearest neighbours (see table 2). Small and large circles stand for Mn^{2+} and O^{2-}, respectively.

are given in table 2. The most interesting feature of this set of parameters is the low value of J_1 (see figure 6) obtained in spite of the fact that normally the ordinary superexchange via one oxygen ion between the Fe^{3+} ions at octahedral and tetrahedral sites of the yttrium–iron garnet is as strong as about 30 K. The low value of J_1 apparently follows from the different distances either side of the intermediate oxygen ion to the nearest magnetic ions: 2.306 Å and 2.422 Å. The second distance is rather long to provide a strong overlap of orbitals. Moreover, it can be

due to the Mn–O–Mn angle, the value of which, 101.3°, is not favourable for superexchange.

Quite an unusual result is the sequence of the values of the exchange parameters J_2, J_3: the further apart the magnetic atoms, the higher the parameter value. Apparently this is because the overlap is stronger if the Mn–O–O–Mn chain is closer to the straight line. The significant difference between J_4 and J_5 for the same coordination sphere also indicates the importance of the superexchange chain geometry.

5. Conclusions

In conclusion, we have studied the spin dynamics of the antiferromagnetic garnet $Mn_3Al_2Ge_3O_{12}$ with magnetic ions Mn^{2+} ($S = 5/2$) in the dodecahedral c sublattice. In spite of there being many (twelve) magnetic ions in the primitive unit cell, a complicated magnetic structure and a low value of the Néel temperature, which taken together make the spin-wave spectrum very complicated, with close-lying branches, we have succeeded in describing it quite well with five statistically significant exchange parameters. They include the interaction between the nearest neighbours via one oxygen ion and all of the interactions with three other coordination spheres. The total number of exchange parameters taken into account is restricted by the number of superexchange paths via two oxygen ions. The values of the exchange parameters indicate the importance of the superexchange chain geometry. The success in the interpretation of the dispersion law of such a complicated system is due to a preliminary modern SW symmetry analysis.

Acknowledgments

We are grateful to B V Mill' (Moscow State University) who provided us with an excellent single crystal of $Mn_3Al_2Ge_3O_{12}$. Four of us (AG, VPP, OPS and YuPCh) thank the ILL for hospitality. Partial support from the Russian Foundation for Fundamental Studies and from the Russian Foundation for Neutron Studies on Condensed Matter is acknowledged.

References

[1] Izyumov Yu A, Naish V E and Ozerov R P 1991 *Neutron Diffraction of Magnetic Materials* (New York: Consultants Bureau)
[2] Bruckel Th, Dorner B, Gukasov A G, Plakhty V P, Prandl W, Shender E F and Smirnov O P 1988 *Z. Phys.* B **72** 477
[3] Plakhty V, Golosovsky I, Gukasov A, Smirnov O, Bruckel Th, Dorner B and Burlet P 1993 *Z. Phys.* B **92** 443
[4] Bruckel Th, Chernenkov Yu, Dorner B, Plakhty V P and Smirnov O P 1990 *Z. Phys.* B **79** 389
[5] Gukasov A G, Bruckel Th, Dorner B, Plakhty V P, Prandl W, Shender E F and Smirnov O P *Europhys. Lett.* **7** 1988 83
[6] Bruckel Th and Prandl W 1988 *Z. Phys.* **73** 57
[7] Golosovsky I V, Plakhty V P and Smirnov O P 1977 *Fiz. Tverd. Tela* **19** 1181
[8] Prandl W 1973 *Phys. Status Solidi* b **55** K159
[9] Izyumov Yu A and Gurin O V 1983 *J. Magn. Magn. Mater.* **36** 226
[10] Izyumov Yu A, Gurin O V and Syromyatnikov V N 1983 *Sov. Phys.–Solid State* **25** 1964
[11] Sikora W, Gurin O V and Syromyatnikov V N 1988 *J. Magn. Magn. Mater.* **71** 255
[12] Kovalev O V 1965 *Irreducible Representation of the Space Groups* (New York: Gordon and Breach)
[13] Valyanskaya T V, Plakhty V P and Sokolov V I 1976 *Sov. Phys.–JETP* **43** 1189
[14] Mill' B V 1975 *Sov. Phys.–Crystallogr.* **19** 653
[15] Prozorova L A, Marchenko V I and Krasnyak Yu V 1985 *JETP Lett.* **41** 637